Temporal Resolution of *nt*PET Using Either Arterial or Reference Region-Derived Plasma Input Functions

Marc D. Normandin, *Student Member*, *IEEE*, and Evan D. Morris, *Member*, *IEEE*

Abstract—We recently introduced an imaging application combining dynamic positron emission tomography (PET), a modification of the two-tissue compartment model, and constrained parameter estimation. The objective of this method, which we have called neurotransmitter PET (*nt*PET), is to estimate the timing of neurotransmitter (NT) kinetics. The time course of NT release in response to drugs or other stimuli may provide information about the function of the brain. In this paper, we evaluate two alternate formulations of *nt*PET, one which uses arterial blood samples as the plasma input function (ART) and another which uses a reference region-derived approximation of the plasma input (REF). Simulated data with strong (moderate noise, prominent NT response) and weak (high noise, subtle NT response) signals were analyzed with *nt*PET using ART and REF. Both methods were able to recover NT profiles resembling the true response, with temporal resolution better than 1 min for strong signals and 3 min for weak signals. Despite potential disadvantages, REF yielded results rivaling those of the ART method. When a sufficiently robust response is anticipated and knowledge of absolute timing is not necessary, the REF method is an appropriate alternative to ART, which is more demanding experimentally.

I. INTRODUCTION

PET imaging using receptor ligands as tracers has been used to detect release of endogenous neurotransmitter (NT) in response to behavioral [1], [2] and pharmacological [3], [4] challenges. For this purpose, we recently introduced an imaging method that combines dynamic PET acquisition, novel compartmental modeling, and constrained parameter estimation, and have called it neurotransmitter PET ("*nt*PET") [5]. By analyzing data from rest (NT level unchanging with time) and activation (NT concentration changing with time due to a stimulus) conditions simultaneously, *nt*PET is able to detect the presence of NT release *and* to characterize its temporal profile. The time course of NT release in response to specific stimuli (e.g., pharmacological or cognitive challenges) may provide information about the function (or dysfunction) of the brain. It has been hypothesized that the timing of NT release

elicited by a drug may be related to the addictiveness of the drug and its potential for abuse [6].

There are two common methods of obtaining the needed plasma input function (PIF) in PET modeling. One is to obtain arterial blood samples, which can be processed to measure the tracer concentration in arterial plasma. The other is to formulate the PIF in terms of PET data from a reference region that has negligible receptor density [7]. Arterial sampling yields an accurate measurement of the true PIF, but requires surgical cannulation of the patient's artery, which introduces considerable complexity into the experiment. Increased cost and invasiveness diminish the practicality of the method. Reference region approaches simplify the experimental procedure and reduce costs and patient discomfort. However, reference methods assume that the reference region PET signal comes solely from free tracer. This is not true early in the scan when considerable tracer remains in the blood.

We have implemented two formulations of *nt*PET, one that uses arterial blood samples (ART) as the PIF and another that uses a reference region-derived approximation (REF) of the PIF. Here, we compare the respective abilities of the ART and REF versions of *nt*PET to accurately and precisely estimate the time course of endogenous NT release from PET data. Using realistic simulations, we seek to determine how the performance of REF compares to that of ART, which we consider to be the gold standard.

II. METHODS

The compartmental model used in *nt*PET [8] is an extension of the standard two-tissue compartment model to include competition between the tracer and an endogenous NT at the receptor sites. Competitive (displaceable) binding is assumed because both tracer and NT bind specifically to a receptor that is limited in number. The model represents mass balances on the tracer and NT as they move between distinct states (i.e., 'Free' in the tissue, 'Bound' to receptors, and in the case of tracer, suspended in 'Plasma'). The rate constants represent the rate of transfer from one compartment to another. These are generally first order (transfer between compartments is a unimolecular event), however the transfer from free to bound is a bimolecular interaction requiring both free ligand (i.e., tracer or NT) and available receptor to occur (binding is saturable). The balance on free tracer, $F(t)$, is

$$\frac{dF(t)}{dt} = K_1 C_P(t) - k_2 F(t)$$
$$- k_{on}\left[B_{max} - B(t) - B^{NT}(t)\right]F(t) + k_{off}B(t) \quad (1)$$

where, in contrast to most PET models, B_{max} is total receptor concentration, including receptors occupied by the NT. Similarly, the balance on bound tracer, $B(t)$, is

$$\frac{dB(t)}{dt} = k_{on}\left[B_{max} - B(t) - B^{NT}(t)\right]F(t) - k_{off}B(t) \quad (2)$$

and the balance on bound NT, $B^{NT}(t)$, is

$$\frac{dB^{NT}(t)}{dt} = k_{on}^{NT}\left[B_{max} - B(t) - B^{NT}(t)\right]F^{NT}(t) - k_{off}^{NT}B^{NT}(t). \quad (3)$$

The output equation relates PET output to the model parameters. The PET signal over a time interval is the sum of the radioactive tracer states weighted by their respective volume fractions, integrated over the frame duration.

$$PET_i = \frac{1}{\Delta t_i}\int_{t_i - \frac{\Delta t_i}{2}}^{t_i + \frac{\Delta t_i}{2}} \varepsilon_V C_{blood}(t) + \varepsilon_T\left[F(t) + B(t)\right]SA(t)dt \quad (4)$$

The specific activity term, $SA(t)$, converts the free and bound states from molecular to radioactive concentrations and accounts for radioactive decay, ε_V is the whole blood volume fraction, and ε_T ($=1 - \varepsilon_V$) is the tissue volume fraction.

The model used by *nt*PET contains two time varying inputs. The first is $C_P(t)$, the concentration of tracer in the plasma. The second input is $F^{NT}(t)$, the concentration of NT free in the tissue. $F^{NT}(t)$ is the quantity of interest, and is estimated in both the ART and REF approaches.

The PIF, $C_P(t)$, is commonly obtained in one of two ways. One is to sample arterial blood and directly measure the tracer concentration in the plasma. The other is to use a reference region, an area which contains a negligible density of the receptors being targeted by the tracer. The equation for this model (Eq. 1 with binding terms omitted) can be rearranged to yield an expression for $C_P(t)$,

$$C_P(t) = \frac{1}{K_1^{REF}}\left[\frac{dF^{REF}(t)}{dt} + k_2^{REF}F^{REF}(t)\right]. \quad (5)$$

Thus the PIF can be approximated from the free tracer in the reference region and its time derivative. We define the ART method as the application of *nt*PET using a PIF obtained from arterial blood samples, and the REF method as the application of *nt*PET when the PIF is derived from the reference region.

The time-varying free NT, $F^{NT}(t)$, is parameterized as a gamma variate function,

$$F^{NT}(t) = Basal + \gamma(t - t_D)^\alpha e^{-\beta(t - t_D)}. \quad (6)$$

Key characteristics are delay time, t_D; peak time, $t_P = t_D + \alpha/\beta$; and peak height, $F^{NT}(t_P)$.

The tracer and NT parameters are estimated by simultaneously fitting the model to dynamic PET data in the rest (constant NT) and activation (time-varying NT) conditions. We assume that tracer parameters will be identical in both conditions, and that the parameters describing NT dynamics will account for differences in data

between conditions not attributable to tracer kinetics.

A. Computer Simulations of PET Data

A canonical set of tracer parameters (i.e., K_1, k_2, k_{on}, k_{off}, B_{max}) was chosen to match the cerebral pharmacokinetics of the PET radioligand [^{11}C]raclopride, a dopamine D_2/D_3 receptor antagonist. Two cases were then considered. In the strong signal case (STRONG), NT parameters (Eq. 6) were selected to approximate the release of dopamine (DA) in response to cocaine (based on [3]), a drug known to cause acute elevation of synaptic DA concentration. Poisson-like noise [9] was added to the simulated data, with variance

$$\sigma_i^2 = \zeta^2 \frac{PET_i}{\Delta t_i} \quad (7)$$

ζ was chosen to yield a signal to noise ratio which meets or exceeds our typical human PET data. In the weak signal case (WEAK), the DA response was more prolonged and of lower magnitude than STRONG. The PET data in WEAK had a higher noise level than in STRONG ($\zeta^2 = 0.015$ in STRONG, $\zeta^2 = 0.03$ in WEAK). Simulations for both cases used DA start times (t_D) of either 5, 10, or 15 minutes after raclopride injection. DA association and dissociation rates were chosen to agree with *in vitro* binding data.

For each value of t_D, 25 data sets were generated for both STRONG and WEAK, each with tracer parameters selected randomly from a ±10% uniform distribution about the canonical parameter set. Each data set was generated by solving the *nt*PET model (Eqs. 1-4, implemented in COMKAT [10]) using a given set of tracer parameters to produce four PET curves. 1. A curve corresponding to the target region during activation. 2. A curve for the target region during rest. 3. A curve for the reference region during activation and, 4. A curve of the reference region during rest. All simulations of activation were made with a given set of tracer parameters and a time varying NT curve (Eq. 6). All rest curves were made with the same parameters but with constant NT. All reference region curves were made with negligible receptors ($B_{max} = 0$).

In order to address the false discovery rate, 50 'null' cases were generated at each noise level used ($\zeta^2 = 0.015, 0.03$). A null case is a set of four curves with constant NT in both the rest and activation conditions.

For all simulations, the PIF was defined according to

$$C_P(t) = (\beta_1 t - \beta_2 - \beta_3)e^{-\kappa_1 t} + \beta_2 e^{-\kappa_2 t} + \beta_3 e^{-\kappa_3 t} \quad (8)$$

with $\beta_1 = 12$, $\beta_2 = 1.8$, $\beta_3 = 0.45$ (nM), $\kappa_1 = 4$, $\kappa_2 = 0.5$, and $\kappa_3 = 0.008$ (min^{-1}) [11]. Tissue fraction (ε_T) and vascular fraction (ε_V) were 0.95 and 0.05, respectively. A sixty minute scan duration was simulated with 60 x 1 min frames.

B. Application of ART and REF methods

Simulated PET data were analyzed using the REF and ART formulations of *nt*PET. Parameter estimation was performed using penalized least squares. The objective function is composed of the weighted residual sum of squares in the rest and activation conditions and two penalty

terms constraining time of peak NT concentration (t_P) and resting binding potential (BP), an index of time-averaged receptor availability. The penalized objective function is

$$\Phi(\Theta_T, \Theta_{NT}) = \sum_i w_i \left[PET_i^{meas} - PET_i(\Theta_T, \Theta_{NT}) \right]^2$$
$$+ \tau_1 \left[\exp\left(-\left[t_P(\Theta_{NT}) - t_L\right]\right) + \exp\left(t_P(\Theta_{NT}) - t_U\right) \right]$$
$$+ \tau_2 \left[BP^{meas} - BP(\Theta_T, \Theta_{NT}) \right]^2 \qquad (9)$$

where w_i are the weights applied to each term (set proportional to σ_i^{-2}), τ_1 and τ_2 are weights applied to the peak time and BP penalty terms ($\tau_1 = \tau_2 = 60$), and t_L and t_U are the upper and lower peak time constraints ($t_L = 0$, $t_U = 60$). $BP(\Theta_T, \Theta_{NT})$ is calculated from the estimated parameters whereas BP^{meas} is determined independently by the Logan graphical method [12]. Eq. 9 is minimized by parameters which fit the data from both scan conditions, yield a BP near BP^{meas}, and find NT events which peak during the scan.

Due to the large number of parameters being estimated, correlation of parameters, and noise in the data, we must be wary of the dependence of our estimates on initial guess. As a precaution, we fit each data set 50 times with 50 randomly chosen initial guesses. Typically, 40 to 45 of the 50 fits converged. Of the fits that converged, the best fits were determined by a multiple stage goodness of fit selection process based on objective criteria [5]. As a result, we obtain multiple answers (typically about 15), representing a family of best NT profiles to explain each pair of scans.

The tracer PIFs (one each for rest and activation conditions) used for REF were derived from the simulated reference region PET data according to Eq. 5. While a noiseless PIF was used to generate simulated data, the plasma inputs used in ART analyses were made noisy according to Eq. 8 to better approximate real data and to allow a fair comparison of between ART and REF.

III. RESULTS

Both the ART and REF methods estimated NT profiles resembling the true, known NT curves, from data of moderate noise level and with prominent NT response (STRONG) and from data with higher noise level and more subtle NT release (WEAK). Estimates of NT timing parameters are shown in Table I for the ART and REF methods applied to STRONG, and in Table II for both methods applied to WEAK, for each of the three different NT curves examined. An example fit and estimated NT curves obtained by application of ART to WEAK are shown in Figure 1. Typical analyses of null data via either method show little or no NT response. Figure 2 shows an ART fit to null data with the same noise level as WEAK.

The precision of estimates is greater and the bias typically less with ART than with REF (Tables I and II). Figure 3 displays a cluster plot of $F^{NT}(t_P)$ plotted against t_P. In analyses of STRONG, we observe scatter in $F^{NT}(t_P)$, however the fits are more consistent in t_P. The ART fits show slightly tighter grouping in t_P than do the REF fits.

TABLE I. DELAY AND PEAK TIME ESTIMATES: STRONG SIGNALS

Delay Time, t_D (minutes)			Peak Time, t_P (minutes)		
	Bias ± SD			Bias ± SD	
TRUE	ART	REF	TRUE	ART	REF
5	-0.39 ± 0.42	-0.42 ± 0.69	12	1.35 ± 0.28	1.59 ± 0.32
10	-0.73 ± 0.43	-0.08 ± 0.64	17	0.98 ± 0.34	1.67 ± 0.39
15	-0.96 ± 0.47	-0.22 ± 0.51	22	1.11 ± 0.33	1.62 ± 0.40

TABLE II. DELAY AND PEAK TIME ESTIMATES: WEAK SIGNALS

Delay Time, t_D (minutes)			Peak Time, t_P (minutes)		
	Bias ± SD			Bias ± SD	
TRUE	ART	REF	TRUE	ART	REF
5	0.05 ± 1.74	1.58 ± 2.40	15	1.92 ± 1.37	2.09 ± 1.45
10	-0.19 ± 2.22	1.10 ± 2.24	20	1.97 ± 1.79	2.78 ± 2.07
15	-0.21 ± 1.81	1.33 ± 2.46	25	1.82 ± 1.59	3.04 ± 2.66

The estimated NT profiles for null data are highly variable in timing parameters, and are consistently of small magnitude. For ART estimates of null data with the same noise level as STRONG, 95% of the estimated NT profiles have average peak height less than 1.16 (fraction of baseline). If we apply ART to data with signal to noise ratio greater or equal to that of STRONG and the resulting average peak height is greater than 1.16, there is reason to believe that the estimated response is not attributable to noise in the data but rather to a bonafide NT response. Similarly, the 95% confidence threshold determined for REF is 1.15 when applied to data with the same noise as that in STRONG. The higher noise level used in WEAK raises the threshold to 1.31 for ART and 1.40 for REF.
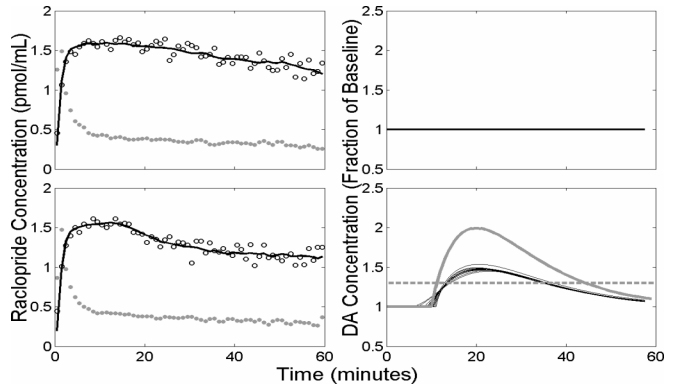

Fig. 1. Example results of WEAK (t_D=10 min) case analyzed with ART. Left panels: simulated PET data (open circles), plasma input (gray circles), and model fit (solid black curve) to the data. Right panels: estimated NT responses (black curves), true NT curve (solid gray), and threshold (dashed gray). Top panels apply to rest condition, bottom panels to activation. REF results are similar.

IV. DISCUSSION

The ART and REF methods differ primarily in how the PIF is determined. In ART, the input is measured directly from blood samples. In REF, the input function is formulated from PET data measured in a receptor-free region assuming that this PET signal is attributable solely to tracer in the free state. This assumption is invalid at early time. The REF method is also more susceptible to noise because its approximation of the PIF requires a time derivative of the reference region data. Finally, REF introduces one net extra parameter to be estimated.
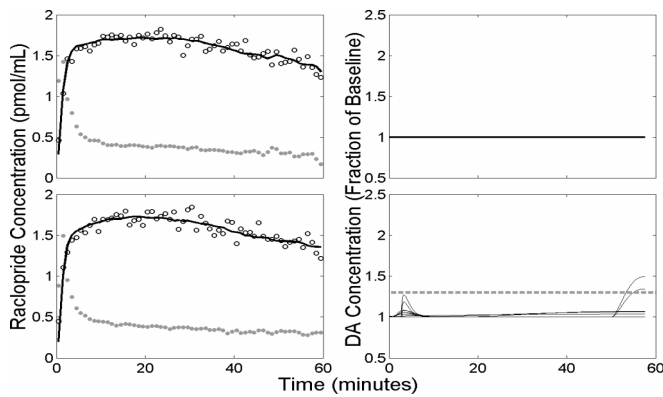
Fig. 2. Example results of null data analyzed with ART, noise level same as WEAK. Left panels: simulated PET data (open circles), plasma input (gray circles), and model fit (solid black curve) to the data. Right panels: estimated NT responses (black curves) and threshold (dashed gray line). Top panels apply to rest condition, bottom panels to activation. REF results are similar.
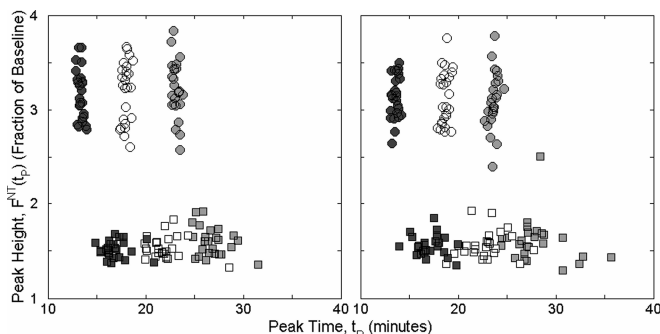

Fig. 3. Estimated peak height of NT response, $F^{NT}(t_P)$, vs. estimated peak time, t_P. ART results are shown on left panel, REF on right panel. Circles indicate results of analyzing STRONG, squares are results of analyzing WEAK. Different colored markers indicate different true NT delay times (dark gray, t_D=5 min; white, t_D=10 min; light gray, t_D=15 min).

We demonstrated that both the REF and ART formulations of *nt*PET can be used to recover the temporal signature of NT release from realistic simulated PET data. In addition to the consistency of our estimated NT responses and their resemblance to the true NT curves used in the simulations, analysis of null case simulations indicates that it is unlikely that we could have obtained our NT estimates by chance. Both methods estimate average peak heights from STRONG signals exceeding their respective thresholds. The peak heights estimated when applied to WEAK approach occasionally fall below the threshold values, suggesting that false negative events may become problematic when magnitude of NT release is small or data are very noisy.

In both ART and REF analyses of STRONG signals, the estimated peak times were more precise and accurate (SD ≤ 0.4 min, bias < 1.7 min) than those estimated from WEAK signals (SD < 2.7 min, bias < 3.1 min), which were noisier and made from smaller NT curves with a poorly defined peak time. Similarly, estimated delay times were less variable; delay bias, however, was slightly greater in ART analyses of STRONG than WEAK. Though we cannot disentangle the effects of increased noise, prolonged endogenous response, and decreased magnitude of NT

release in these studies, we observe that the performance of both versions of *nt*PET degrades as the quality of data and prominence of the NT response diminish.

V. CONCLUSIONS

We compared two versions of *nt*PET, which differ in how the plasma input function is determined. In spite of potential disadvantages, the REF method is nearly as successful as ART in recovering NT profiles from either STRONG or WEAK signals. Both methods demonstrate temporal resolution better than one minute for STRONG signals and three minutes for WEAK signals. In applications where we anticipate a sufficient effect size and do not need to know *absolute* timing of the NT response, the more convenient REF method is probably preferred.

REFERENCES

[1] M. J. Koepp, R. N. Gunn, A. D. Lawrence, V. J. Cunningham, A. Dagher, T. Jones, D. J. Brooks, C. J. Bench, and P. M. Grasby, "Evidence for striatal dopamine release during a video game," *Nature*, vol. 393, no. 6682, pp. 266-268, May1998.

[2] R. D. Badgaiyan, A. J. Fischman, and N. M. Alpert, "Striatal dopamine release during unrewarded motor task in human volunteers," *Neuroreport*, vol. 14, no. 11, pp. 1421-1424, Aug.2003.

[3] N. D. Volkow, J. S. Fowler, S. J. Gatley, S. L. Dewey, G. J. Wang, J. Logan, Y. S. Ding, D. Franceschi, A. Gifford, A. Morgan, N. Pappas, and P. King, "Comparable changes in synaptic dopamine induced by methylphenidate and by cocaine in the baboon brain," *Synapse*, vol. 31, no. 1, pp. 59-66, Jan.1999.

[4] I. Boileau, J. M. Assaad, R. O. Pihl, C. Benkelfat, M. Leyton, M. Diksic, R. E. Tremblay, and A. Dagher, "Alcohol promotes dopamine release in the human nucleus accumbens," *Synapse*, vol. 49, no. 4, pp. 226-231, Sept.2003.

[5] E. D. Morris, K. K. Yoder, C. Wang, M. D. Normandin, Q. H. Zheng, B. Mock, R. F. Muzic, Jr., and J. C. Froehlich, "ntPET: a new application of PET imaging for characterizing the kinetics of endogenous neurotransmitter release," *Mol. Imaging*, vol. 4, no. 4, pp. 473-489, Oct.2005.

[6] N. D. Volkow and J. M. Swanson, "Variables That Affect the Clinical Use and Abuse of Methylphenidate in the Treatment of ADHD," *Amer J of Psychiatry*, vol. 160, no. 11, pp. 1909-1918, Nov.2003.

[7] V. J. Cunningham, S. P. Hume, G. R. Price, R. G. Ahier, J. E. Cremer, and A. K. Jones, "Compartmental analysis of diprenorphine binding to opiate receptors in the rat in vivo and its comparison with equilibrium data in vitro," *J Cereb. Blood Flow Metab*, vol. 11, no. 1, pp. 1-9, Jan.1991.

[8] E. D. Morris, R. E. Fischer, N. M. Alpert, S. L. Rauch, and A. J. Fischman, "In vivo imaging of neuromodulation using positron emission tomography: Optimal ligand characteristics and task length for detection of activation," *Hum Brain Map.*, vol. 3, pp. 35-55, 1995.

[9] E. M. Landaw and J. J. DiStefano, III, "Multiexponential, multicompartmental, and noncompartmental modeling. II. Data analysis and statistical considerations," *Am J Physiol Regul Integr Comp Physiol*, vol. 246, no. 5, p. R665-R677, May1984.

[10] R. F. Muzic, Jr. and S. Cornelius, "COMKAT: Compartment Model Kinetic Analysis Tool," *J Nucl Med*, vol. 42, no. 4, pp. 636-645, Apr.2001.

[11] D. Feng, S. C. Huang, and X. Wang, "Models for computer simulation studies of input functions for tracer kinetic modeling with positron emission tomography," *Int. J Biomed. Comput.*, vol. 32, no. 2, pp. 95-110, Mar.1993.

[12] J. Logan, J. S. Fowler, N. D. Volkow, G. J. Wang, Y. S. Ding, and D. L. Alexoff, "Distribution Volume Ratios Without Blood Sampling from Graphical Analysis of PET Data," *J Cereb. Blood Flow Metab*, vol. 16, no. 5, pp. 834-840, Sept.1996.